BABAR-CONF-01/10
SLAC-PUB-8926
hep-ex/0107058
July, 2001

Measurements of B^0 decays to $\pi^+\pi^-\pi^0$

The *BABAR* Collaboration

July 21, 2001

Abstract

We present preliminary results of searches for exclusive B^0 decays to $\pi^+\pi^-\pi^0$ among 22.7 million $b\overline{b}$ pairs collected by the *BABAR* experiment from electron-positron collisions near the $\Upsilon(4S)$ resonance. We measure $\mathcal{B}(B^0 \to \rho^{\mp}\pi^{\pm}) = (28.9 \pm 5.4 \pm 4.3) \times 10^{-6}$, and find no evidence for the presence of any other decay mode in the $\pi^+\pi^-\pi^0$ Dalitz plot. Upper limits are determined for the branching fractions of $B^0 \to \rho^0\pi^0$, non-resonant B^0 decays to $\pi^+\pi^-\pi^0$ and of several discrete regions of $\pi^+\pi^-\pi^0$ phase-space. We also measure the direct CP-violating asymmetry between the rates of untagged $\rho^+\pi^-$ and $\rho^-\pi^+$, finding no significant evidence for an effect.

Submitted to the
20^{th} International Symposium on Lepton and Photon Interactions at High Energies,
7/23—7/28/2001, Rome, Italy

Stanford Linear Accelerator Center, Stanford University, Stanford, CA 94309

Work supported in part by Department of Energy contract DE-AC03-76SF00515.

The *BABAR* Collaboration,

B. Aubert, D. Boutigny, J.-M. Gaillard, A. Hicheur, Y. Karyotakis, J. P. Lees, P. Robbe, V. Tisserand

Laboratoire de Physique des Particules, F-74941 Annecy-le-Vieux, France

A. Palano

Università di Bari, Dipartimento di Fisica and INFN, I-70126 Bari, Italy

G. P. Chen, J. C. Chen, N. D. Qi, G. Rong, P. Wang, Y. S. Zhu

Institute of High Energy Physics, Beijing 100039, China

G. Eigen, P. L. Reinertsen, B. Stugu

University of Bergen, Inst. of Physics, N-5007 Bergen, Norway

B. Abbott, G. S. Abrams, A. W. Borgland, A. B. Breon, D. N. Brown, J. Button-Shafer, R. N. Cahn, A. R. Clark, M. S. Gill, A. V. Gritsan, Y. Groysman, R. G. Jacobsen, R. W. Kadel, J. Kadyk, L. T. Kerth, S. Kluth, Yu. G. Kolomensky, J. F. Kral, C. LeClerc, M. E. Levi, T. Liu, G. Lynch, A. B. Meyer, M. Momayezi, P. J. Oddone, A. Perazzo, M. Pripstein, N. A. Roe, A. Romosan, M. T. Ronan, V. G. Shelkov, A. V. Telnov, W. A. Wenzel

Lawrence Berkeley National Laboratory and University of California, Berkeley, CA 94720, USA

P. G. Bright-Thomas, T. J. Harrison, C. M. Hawkes, D. J. Knowles, S. W. O'Neale, R. C. Penny, A. T. Watson, N. K. Watson

University of Birmingham, Birmingham, B15 2TT, United Kingdom

T. Deppermann, K. Goetzen, H. Koch, J. Krug, M. Kunze, B. Lewandowski, K. Peters, H. Schmuecker, M. Steinke

Ruhr Universität Bochum, Institut für Experimentalphysik 1, D-44780 Bochum, Germany

J. C. Andress, N. R. Barlow, W. Bhimji, N. Chevalier, P. J. Clark, W. N. Cottingham, N. De Groot, N. Dyce, B. Foster, J. D. McFall, D. Wallom, F. F. Wilson

University of Bristol, Bristol BS8 1TL, United Kingdom

K. Abe, C. Hearty, T. S. Mattison, J. A. McKenna, D. Thiessen

University of British Columbia, Vancouver, BC, Canada V6T 1Z1

S. Jolly, A. K. McKemey, J. Tinslay

Brunel University, Uxbridge, Middlesex UB8 3PH, United Kingdom

V. E. Blinov, A. D. Bukin, D. A. Bukin, A. R. Buzykaev, V. B. Golubev, V. N. Ivanchenko, A. A. Korol, E. A. Kravchenko, A. P. Onuchin, A. A. Salnikov, S. I. Serednyakov, Yu. I. Skovpen, V. I. Telnov, A. N. Yushkov

Budker Institute of Nuclear Physics, Novosibirsk 630090, Russia

D. Best, A. J. Lankford, M. Mandelkern, S. McMahon, D. P. Stoker

University of California at Irvine, Irvine, CA 92697, USA

A. Ahsan, K. Arisaka, C. Buchanan, S. Chun

University of California at Los Angeles, Los Angeles, CA 90024, USA

J. G. Branson, D. B. MacFarlane, S. Prell, Sh. Rahatlou, G. Raven, V. Sharma

University of California at San Diego, La Jolla, CA 92093, USA

C. Campagnari, B. Dahmes, P. A. Hart, N. Kuznetsova, S. L. Levy, O. Long, A. Lu, J. D. Richman, W. Verkerke, M. Witherell, S. Yellin

University of California at Santa Barbara, Santa Barbara, CA 93106, USA

J. Beringer, D. E. Dorfan, A. M. Eisner, A. Frey, A. A. Grillo, M. Grothe, C. A. Heusch, R. P. Johnson, W. Kroeger, W. S. Lockman, T. Pulliam, H. Sadrozinski, T. Schalk, R. E. Schmitz, B. A. Schumm, A. Seiden, M. Turri, W. Walkowiak, D. C. Williams, M. G. Wilson

University of California at Santa Cruz, Institute for Particle Physics, Santa Cruz, CA 95064, USA

E. Chen, G. P. Dubois-Felsmann, A. Dvoretskii, D. G. Hitlin, S. Metzler, J. Oyang, F. C. Porter, A. Ryd, A. Samuel, M. Weaver, S. Yang, R. Y. Zhu

California Institute of Technology, Pasadena, CA 91125, USA

S. Devmal, T. L. Geld, S. Jayatilleke, G. Mancinelli, B. T. Meadows, M. D. Sokoloff

University of Cincinnati, Cincinnati, OH 45221, USA

T. Barillari, P. Bloom, M. O. Dima, S. Fahey, W. T. Ford, D. R. Johnson, U. Nauenberg, A. Olivas, H. Park, P. Rankin, J. Roy, S. Sen, J. G. Smith, W. C. van Hoek, D. L. Wagner

University of Colorado, Boulder, CO 80309, USA

J. Blouw, J. L. Harton, M. Krishnamurthy, A. Soffer, W. H. Toki, R. J. Wilson, J. Zhang

Colorado State University, Fort Collins, CO 80523, USA

T. Brandt, J. Brose, T. Colberg, G. Dahlinger, M. Dickopp, R. S. Dubitzky, A. Hauke, E. Maly, R. Müller-Pfefferkorn, S. Otto, K. R. Schubert, R. Schwierz, B. Spaan, L. Wilden

Technische Universität Dresden, Institut für Kern- und Teilchenphysik, D-01062, Dresden, Germany

L. Behr, D. Bernard, G. R. Bonneaud, F. Brochard, J. Cohen-Tanugi, S. Ferrag, E. Roussot, S. T'Jampens, Ch. Thiebaux, G. Vasileiadis, M. Verderi

Ecole Polytechnique, F-91128 Palaiseau, France

A. Anjomshoaa, R. Bernet, A. Khan, D. Lavin, F. Muheim, S. Playfer, J. E. Swain

University of Edinburgh, Edinburgh EH9 3JZ, United Kingdom

M. Falbo

Elon University, Elon University, NC 27244-2010, USA

C. Borean, C. Bozzi, S. Dittongo, M. Folegani, L. Piemontese

Università di Ferrara, Dipartimento di Fisica and INFN, I-44100 Ferrara, Italy

E. Treadwell

Florida A&M University, Tallahassee, FL 32307, USA

F. Anulli,[1] R. Baldini-Ferroli, A. Calcaterra, R. de Sangro, D. Falciai, G. Finocchiaro, P. Patteri, I. M. Peruzzi,[2]1 M. Piccolo, Y. Xie, A. Zallo

Laboratori Nazionali di Frascati dell'INFN, I-00044 Frascati, Italy

[1]Also with Università di Perugia, I-06100 Perugia, Italy

S. Bagnasco, A. Buzzo, R. Contri, G. Crosetti, P. Fabbricatore, S. Farinon, M. Lo Vetere, M. Macri, M. R. Monge, R. Musenich, M. Pallavicini, R. Parodi, S. Passaggio, F. C. Pastore, C. Patrignani, M. G. Pia, C. Priano, E. Robutti, A. Santroni

Università di Genova, Dipartimento di Fisica and INFN, I-16146 Genova, Italy

M. Morii

Harvard University, Cambridge, MA 02138, USA

R. Bartoldus, T. Dignan, R. Hamilton, U. Mallik

University of Iowa, Iowa City, IA 52242, USA

J. Cochran, H. B. Crawley, P.-A. Fischer, J. Lamsa, W. T. Meyer, E. I. Rosenberg

Iowa State University, Ames, IA 50011-3160, USA

M. Benkebil, G. Grosdidier, C. Hast, A. Höcker, H. M. Lacker, S. Laplace, V. Lepeltier, A. M. Lutz, S. Plaszczynski, M. H. Schune, S. Trincaz-Duvoid, A. Valassi, G. Wormser

Laboratoire de l'Accélérateur Linéaire, F-91898 Orsay, France

R. M. Bionta, V. Brigljević , D. J. Lange, M. Mugge, X. Shi, K. van Bibber, T. J. Wenaus, D. M. Wright, C. R. Wuest

Lawrence Livermore National Laboratory, Livermore, CA 94550, USA

M. Carroll, J. R. Fry, E. Gabathuler, R. Gamet, M. George, M. Kay, D. J. Payne, R. J. Sloane, C. Touramanis

University of Liverpool, Liverpool L69 3BX, United Kingdom

M. L. Aspinwall, D. A. Bowerman, P. D. Dauncey, U. Egede, I. Eschrich, N. J. W. Gunawardane, J. A. Nash, P. Sanders, D. Smith

University of London, Imperial College, London, SW7 2BW, United Kingdom

D. E. Azzopardi, J. J. Back, P. Dixon, P. F. Harrison, R. J. L. Potter, H. W. Shorthouse, P. Strother, P. B. Vidal, M. I. Williams

Queen Mary, University of London, E1 4NS, United Kingdom

G. Cowan, S. George, M. G. Green, A. Kurup, C. E. Marker, P. McGrath, T. R. McMahon, S. Ricciardi, F. Salvatore, I. Scott, G. Vaitsas

University of London, Royal Holloway and Bedford New College, Egham, Surrey TW20 0EX, United Kingdom

D. Brown, C. L. Davis

University of Louisville, Louisville, KY 40292, USA

J. Allison, R. J. Barlow, J. T. Boyd, A. C. Forti, J. Fullwood, F. Jackson, G. D. Lafferty, N. Savvas, E. T. Simopoulos, J. H. Weatherall

University of Manchester, Manchester M13 9PL, United Kingdom

A. Farbin, A. Jawahery, V. Lillard, J. Olsen, D. A. Roberts, J. R. Schieck

University of Maryland, College Park, MD 20742, USA

G. Blaylock, C. Dallapiccola, K. T. Flood, S. S. Hertzbach, R. Kofler, T. B. Moore, H. Staengle, S. Willocq

University of Massachusetts, Amherst, MA 01003, USA

B. Brau, R. Cowan, G. Sciolla, F. Taylor, R. K. Yamamoto
Massachusetts Institute of Technology, Laboratory for Nuclear Science, Cambridge, MA 02139, USA

M. Milek, P. M. Patel, J. Trischuk
McGill University, Montréal, Canada QC H3A 2T8

F. Lanni, F. Palombo
Università di Milano, Dipartimento di Fisica and INFN, I-20133 Milano, Italy

J. M. Bauer, M. Booke, L. Cremaldi, V. Eschenburg, R. Kroeger, J. Reidy, D. A. Sanders, D. J. Summers
University of Mississippi, University, MS 38677, USA

J. P. Martin, J. Y. Nief, R. Seitz, P. Taras, A. Woch, V. Zacek
Université de Montréal, Laboratoire René J. A. Lévesque, Montréal, Canada QC H3C 3J7

H. Nicholson, C. S. Sutton
Mount Holyoke College, South Hadley, MA 01075, USA

C. Cartaro, N. Cavallo,[3] G. De Nardo, F. Fabozzi, C. Gatto, L. Lista, P. Paolucci, D. Piccolo, C. Sciacca
Università di Napoli Federico II, Dipartimento di Scienze Fisiche and INFN, I-80126, Napoli, Italy

J. M. LoSecco
University of Notre Dame, Notre Dame, IN 46556, USA

J. R. G. Alsmiller, T. A. Gabriel, T. Handler
Oak Ridge National Laboratory, Oak Ridge, TN 37831, USA

J. Brau, R. Frey, M. Iwasaki, N. B. Sinev, D. Strom
University of Oregon, Eugene, OR 97403, USA

F. Colecchia, F. Dal Corso, A. Dorigo, F. Galeazzi, M. Margoni, G. Michelon, M. Morandin, M. Posocco, M. Rotondo, F. Simonetto, R. Stroili, E. Torassa, C. Voci
Università di Padova, Dipartimento di Fisica and INFN, I-35131 Padova, Italy

M. Benayoun, H. Briand, J. Chauveau, P. David, Ch. de la Vaissière, L. Del Buono, O. Hamon, F. Le Diberder, Ph. Leruste, J. Lory, L. Roos, J. Stark, S. Versillé
Universités Paris VI et VII, Lab de Physique Nucléaire H. E., F-75252 Paris, France

P. F. Manfredi, V. Re, V. Speziali
Università di Pavia, Dipartimento di Elettronica and INFN, I-27100 Pavia, Italy

E. D. Frank, L. Gladney, Q. H. Guo, J. H. Panetta
University of Pennsylvania, Philadelphia, PA 19104, USA

C. Angelini, G. Batignani, S. Bettarini, M. Bondioli, M. Carpinelli, F. Forti, M. A. Giorgi, A. Lusiani, F. Martinez-Vidal, M. Morganti, N. Neri, E. Paoloni, M. Rama, G. Rizzo, F. Sandrelli, G. Simi, G. Triggiani, J. Walsh
Università di Pisa, Scuola Normale Superiore and INFN, I-56010 Pisa, Italy

[3]Also with Università della Basilicata, I-85100 Potenza, Italy

M. Haire, D. Judd, K. Paick, L. Turnbull, D. E. Wagoner

Prairie View A&M University, Prairie View, TX 77446, USA

J. Albert, C. Bula, P. Elmer, C. Lu, K. T. McDonald, V. Miftakov, S. F. Schaffner, A. J. S. Smith, A. Tumanov, E. W. Varnes

Princeton University, Princeton, NJ 08544, USA

G. Cavoto, D. del Re, R. Faccini,[4] F. Ferrarotto, F. Ferroni, K. Fratini, E. Lamanna, E. Leonardi, M. A. Mazzoni, S. Morganti, G. Piredda, F. Safai Tehrani, M. Serra, C. Voena

Università di Roma La Sapienza, Dipartimento di Fisica and INFN, I-00185 Roma, Italy

S. Christ, R. Waldi

Universität Rostock, D-18051 Rostock, Germany

P. F. Jacques, M. Kalelkar, R. J. Plano

Rutgers University, New Brunswick, NJ 08903, USA

T. Adye, B. Franek, N. I. Geddes, G. P. Gopal, S. M. Xella

Rutherford Appleton Laboratory, Chilton, Didcot, Oxon, OX11 0QX, United Kingdom

R. Aleksan, G. De Domenico, S. Emery, A. Gaidot, S. F. Ganzhur, P.-F. Giraud, G. Hamel de Monchenault, W. Kozanecki, M. Langer, G. W. London, B. Mayer, B. Serfass, G. Vasseur, Ch. Yèche, M. Zito

DAPNIA, Commissariat à l'Energie Atomique/Saclay, F-91191 Gif-sur-Yvette, France

N. Copty, M. V. Purohit, H. Singh, F. X. Yumiceva

University of South Carolina, Columbia, SC 29208, USA

I. Adam, P. L. Anthony, D. Aston, K. Baird, J. P. Berger, E. Bloom, A. M. Boyarski, F. Bulos, G. Calderini, R. Claus, M. R. Convery, D. P. Coupal, D. H. Coward, J. Dorfan, M. Doser, W. Dunwoodie, R. C. Field, T. Glanzman, G. L. Godfrey, S. J. Gowdy, P. Grosso, T. Himel, T. Hryn'ova, M. E. Huffer, W. R. Innes, C. P. Jessop, M. H. Kelsey, P. Kim, M. L. Kocian, U. Langenegger, D. W. G. S. Leith, S. Luitz, V. Luth, H. L. Lynch, H. Marsiske, S. Menke, R. Messner, K. C. Moffeit, R. Mount, D. R. Muller, C. P. O'Grady, M. Perl, S. Petrak, H. Quinn, B. N. Ratcliff, S. H. Robertson, L. S. Rochester, A. Roodman, T. Schietinger, R. H. Schindler, J. Schwiening, V. V. Serbo, A. Snyder, A. Soha, S. M. Spanier, J. Stelzer, D. Su, M. K. Sullivan, H. A. Tanaka, J. Va'vra, S. R. Wagner, A. J. R. Weinstein, W. J. Wisniewski, D. H. Wright, C. C. Young

Stanford Linear Accelerator Center, Stanford, CA 94309, USA

P. R. Burchat, C. H. Cheng, D. Kirkby, T. I. Meyer, C. Roat

Stanford University, Stanford, CA 94305-4060, USA

R. Henderson

TRIUMF, Vancouver, BC, Canada V6T 2A3

W. Bugg, H. Cohn, A. W. Weidemann

University of Tennessee, Knoxville, TN 37996, USA

[4]Also with University of California at San Diego, La Jolla, CA 92093, USA

J. M. Izen, I. Kitayama, X. C. Lou, M. Turcotte
University of Texas at Dallas, Richardson, TX 75083, USA

F. Bianchi, M. Bona, B. Di Girolamo, D. Gamba, A. Smol, D. Zanin
Università di Torino, Dipartimento di Fisica Sperimentale and INFN, I-10125 Torino, Italy

L. Bosisio, G. Della Ricca, L. Lanceri, A. Pompili, P. Poropat, M. Prest, E. Vallazza, G. Vuagnin
Università di Trieste, Dipartimento di Fisica and INFN, I-34127 Trieste, Italy

R. S. Panvini
Vanderbilt University, Nashville, TN 37235, USA

C. M. Brown, A. De Silva, R. Kowalewski, J. M. Roney
University of Victoria, Victoria, BC, Canada V8W 3P6

H. R. Band, E. Charles, S. Dasu, F. Di Lodovico, A. M. Eichenbaum, H. Hu, J. R. Johnson, R. Liu, J. Nielsen, Y. Pan, R. Prepost, I. J. Scott, S. J. Sekula, J. H. von Wimmersperg-Toeller, S. L. Wu, Z. Yu, H. Zobernig
University of Wisconsin, Madison, WI 53706, USA

T. M. B. Kordich, H. Neal
Yale University, New Haven, CT 06511, USA

1 Introduction

We describe the measurement of branching fractions for B^0 decays[1] to the final state $\pi^+\pi^-\pi^0$. We include here those decays which proceed through a resonant, quasi-two body intermediate state, as well as non-resonant three-body decays with which they interfere.

The intrinsic interest in these modes stems from their potential use for measuring the angle α of the unitarity triangle [1]. Such measurements would exploit interference between the $B^0 \to \rho^{\mp}\pi^{\pm}$ modes and the colour-suppressed $B^0 \to \rho^0\pi^0$ mode. However, the former modes were discovered only in 1999 [2], and the latter mode remains undiscovered. Furthermore, the proposed measurement of α assumes that only the lowest-mass ρ mesons contribute to the $\pi^+\pi^-\pi^0$ Dalitz plot, an assumption that needs to be tested. It has also been suggested [3, 4] that resonances with quantum numbers other than those of the ρ might make significant contributions to the rate in the Dalitz plot, and it is important also to search for these. In the analyses presented here, we improve on earlier measurements of $B^0 \to \rho^{\mp}\pi^{\pm}$ and search for $B^0 \to \rho^0\pi^0$ modes containing other resonances, and non-resonant $B^0 \to \pi^+\pi^-\pi^0$ decays.

2 The *BABAR* Detector and Dataset

The data used in these analyses were collected with the *BABAR* detector at the PEP-II storage ring. The *BABAR* detector, described in detail elsewhere [5], consists of five active sub-detectors. Surrounding the beam-pipe is a silicon vertex tracker (SVT) to track particles of momentum less than $\sim$120 MeV/c and to provide precision measurements of the positions of charged particles of all momenta as they leave the interaction point. A beam-support tube surrounds the SVT. Outside this is a 40-layer drift chamber (DCH), filled with an 80:20 helium-isobutane gas mixture to minimize multiple scattering, providing measurements of track momenta in a 1.5 T magnetic field. It also provides energy-loss measurements that contribute to charged particle identification. Surrounding the outer circumference of the drift chamber is a novel detector of internally reflected Cherenkov radiation (DIRC) that provides charged hadron identification in the barrel region. This consists of quartz bars of refractive index $\sim$1.42 in which Cherenkov light is produced by relativistic charged particles. This is internally reflected and collected by an array of photomultiplier tubes, which enable Cherenkov rings to be reconstructed and associated with the charged tracks in the DCH, providing a measurement of particle velocities. Outside the DIRC is a CsI(Tl) electromagnetic calorimeter (EMC) which is used to detect photons and neutral hadrons, and to provide electron identification. The EMC is surrounded by a superconducting coil which provides the magnetic field for tracking. Outside the coil, the flux return is instrumented with resistive plate chambers interspersed with iron.

The data sample used for the analyses contains 22.74 million $B\overline{B}$ pairs [5], corresponding to 20.7 fb^{-1} taken on the Υ(4S) resonance. In addition, 2.6 fb^{-1} of data taken off-resonance have been used to validate the contribution to backgrounds resulting from e^+e^- annihilation into light $q\overline{q}$ pairs. These data have all been processed with reconstruction software to determine the three-momenta and positions of charged tracks and the energies and positions of photons. Refined information on particle type from the various sub-detectors described above is also provided, and is used in particle identification algorithms in the analyses.

[1] Charge conjugate initial and final states are assumed everywhere unless otherwise stated.

3 Analysis Method

3.1 Dalitz Plot Decomposition for $\pi^+\pi^-\pi^0$

Data for the $B^0 \to \pi^+\pi^-\pi^0$ final state can be represented on a Dalitz plot. A complete picture of the Dalitz plot structure can be obtained only by performing an amplitude analysis, but the simplest such analysis uses eight parameters [6], and would be difficult with the relatively low statistics currently available. Previous analyses of such decays in this and other experiments [2, 7, 8] have focused predominantly on resonant quasi two-body decays to $\rho(770)\pi$, in which the data are localised in bands within the Dalitz plot. We follow this approach, except that our current statistics are sufficient to allow also searches for higher resonances populating different bands in the Dalitz plot. We therefore sub-divide the Dalitz plot into several distinct regions, each of which is chosen to be sensitive primarily to a single resonance, such as the $\rho(770)$, $\rho(1450)$ and $f_0(400-1200)$ (also called σ), and we perform an independent search in each. In addition, we consider the middle part of the Dalitz plot, which is sensitive to non-resonant decays. We have found that the measured background level varies dramatically across the Dalitz plot and our approach allows the analysis for each resonance to be optimised independently, taking into account the local background level. The seven regions are indicated in Fig. 1. The regions are defined using selection criteria for the

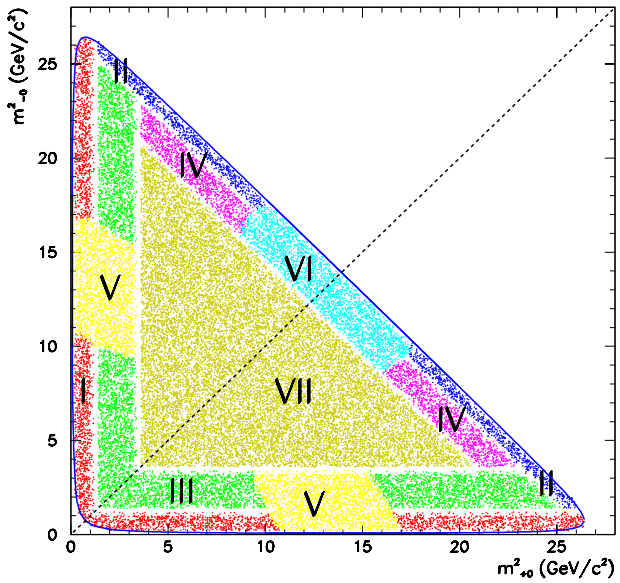

Figure 1: The branching fraction into the Dalitz plot is measured in separate regions which are sensitive to the following modes: I: $B^0 \to \rho^\mp\pi^\pm$, II: $B^0 \to \rho^0\pi^0$, III: $B^0 \to \rho'^\mp\pi^\pm$, IV: $B^0 \to \rho'^0\pi^0$, V: $B^0 \to$ charged scalar and $\pi^\mp$, VI: $B^0 \to$ neutral scalar and π^0, VII: $B^0 \to \pi^+\pi^-\pi^0$ at high mass. The dashed line along the diagonal represents the *CP*-symmetry axis.

invariant mass of $\pi\pi$-pair combinations, $m_{\pi\pi}$, and the pair helicity angle, θ_H, defined as the angle between the direction of one of the pions and the direction of the parent B meson candidate, computed in the $\pi\pi$-pair rest frame. The region definitions are summarised in Table 1.

Table 1: Regions of the $B^0 \to \pi^+\pi^-\pi^0$ Dalitz plot: the regions are kinematically-defined by the $m_{\pi\pi}$ and $|\cos(\theta_H)|$ selection criteria. Any possibly dominant resonance is noted for each region.

Region	Putative dominant resonance	$m_{\pi\pi}(\,\mathrm{GeV}/c^2)$ and $\lvert\cos(\theta_H)\rvert$ selection
I	$\rho^{\pm}(770)$	$0.52 < m_{\pi^+\pi^0} < 1.02$ and $\lvert\cos(\theta_H^{+0})\rvert > 0.25$ $0.52 < m_{\pi^-\pi^0} < 1.02$ and $\lvert\cos(\theta_H^{-0})\rvert > 0.25$
II	$\rho^0(770)$	$0.57 < m_{\pi^+\pi^-} < 1.02$ and $\lvert\cos(\theta_H^{\pm})\rvert > 0.3$ and $m_{\pi^+\pi^0} > 1.2$ and $m_{\pi^-\pi^0} > 1.2$
III	$\rho^{\pm}(1450)$	$m_{\pi^+\pi^0}$ and $m_{\pi^-\pi^0}$ and $m_{\pi^+\pi^-} > 1.2$ and $((m_{\pi^+\pi^0} < 1.8$ and $\lvert\cos(\theta_H^{+0})\rvert > 0.25)$ or $(m_{\pi^-\pi^0} < 1.8$ and $\lvert\cos(\theta_H^{-0})\rvert > 0.25))$
IV	$\rho^0(1450)$	$1.2 < m_{\pi^+\pi^-} < 1.8$ and $\lvert\cos\theta_H^{+-}\rvert > 0.3$ and $m_{\pi^+\pi^0}$ and $m_{\pi^-\pi^0} > 1.9$
V	charged scalar	$(0.52 < m_{\pi^+\pi^0} < 1.8$ and $\lvert\cos(\theta_H^{+0})\rvert < 0.25)$ or $(0.52 < m_{\pi^-\pi^0} < 1.8$ and $\lvert\cos(\theta_H^{-0})\rvert < 0.25)$
VI	$f^0(400-1200)$	$0.57 < m_{\pi^+\pi^-} < 1.8$ and $\lvert\cos(\theta_H^{+-})\rvert < 0.30$
VII	high mass(> 1900)	$m^2_{\pi^+\pi^0}$ and $m^2_{\pi^-\pi^0}$ and $m^2_{\pi^+\pi^-} > 0.13\ m_B^2$

3.2 Candidate Selection

Charged tracks are required to have a momentum less than $10\,\mathrm{GeV}/c$ and a transverse momentum greater than $0.1\,\mathrm{GeV}/c$. They are required to have at least 20 hits in the DCH and to originate close to the beam-spot. In addition, $\pi^{\pm}$ candidates are selected as those charged tracks which are unlikely to be kaons, based on Cherenkov angle information from the DIRC combined with energy-loss information from the DCH.

Photon candidates are identified in the calorimeter as deposits of energy unassociated with charged tracks. π^0s are reconstructed by combining pairs of photon candidates and requiring that the invariant mass of the resultant candidate is between $100\,\mathrm{MeV}/c^2$ and $160\,\mathrm{MeV}/c^2$. Photon candidates used in π^0 reconstruction are required to have a minimum energy of 30 MeV and a shower shape consistent with a photon.

Reconstruction of B candidates is accomplished by forming all combinations of $\pi^+\pi^-\pi^0$ candidates in each event and applying a loose quality requirement of $\chi^2 < 200$ to the fitted vertex for the $\pi^+\pi^-$ pair. The B candidates are required to satisfy kinematic constraints appropriate for B mesons. We use two kinematic variables [5] for this: $m_{\mathrm{ES}} = \sqrt{(\frac{1}{2}s + \mathbf{p}_0\cdot\mathbf{p}_B)^2/E_0^2 - p_B^2}$, where the subscripts 0 and B refer to the e^+e^- system and the B candidate, respectively; and $\Delta E = E_B^* - \sqrt{s}/2$, where E_B^* is the B candidate energy in the center-of-mass frame. For signal events, the former has a value close to the B meson mass and the latter should be close to zero.

The selection criteria in each region are optimized for sensitivity to the branching fraction. The criteria that are allowed to vary are the mass requirements on the π^0 and $\rho(770)$ candidates, $\cos\theta_H$, and the requirements on event shape discussed in the following section.

3.3 Background Suppression and Characterisation

Charmless hadronic modes suffer very large amounts of background from random combinations of tracks, mostly from light quark and charm continuum production. Such backgrounds may be reduced by selection requirements on the event topologies computed in the $\Upsilon(4S)$ rest frame. We use $\cos\theta_T$, the cosine of the angle θ_T between the thrust axis of the B meson decay and the thrust axis of the rest of the event. For continuum-related backgrounds, these two directions tend to be aligned because the reconstructed B candidate daughters generally lie in the same jets as those in the rest of the event. By contrast, in B events, the decay products from one B meson are independent of those in the other, making the distribution of this angle isotropic. In consequence, requiring that this opening angle be significant provides a strong suppression of continuum backgrounds.

Other event shape variables also help to separate signal and background. We form a linear combination of 11 variables in a Fisher discriminant $\mathcal{F}$ [9]. The coefficients for each variable are chosen to maximize the separation between training samples of signal and background events. The variables contained in $\mathcal{F}$ are:

- the cosine of the angle between the B momentum and the beam axis;
- the cosine of the angle between the thrust axis of the B candidate and the beam axis; and
- the summed momentum, in nine cones coaxial with the thrust axis of the B candidate, of all detected particles in the event that are not associated with the B decay.

Despite the power of such topological variables to reduce the combinatorial backgrounds, most of the modes we have searched for continue to suffer significant background levels. Even after stringent selection criteria have been applied, it is necessary to make a background subtraction to isolate a signal or set an upper limit. In order to do this, the background in the signal region is estimated from the number of events in a sideband region, located near the signal region in the $m_{\rm ES}$-ΔE plane, and extrapolated into the signal region. The shape of the distribution of the background as a function of $m_{\rm ES}$ is parameterised according to the ARGUS function [10], and is measured using on-resonance data slightly displaced from the signal region in the ΔE variable ($0.1 < |\Delta E\,| < 0.25$). We define $\mathcal{R}$ to be the ratio of the number of candidates in the signal region to the number in the sideband region. Off-resonance data yields a consistent ratio and is averaged with the result measured on-resonance. We measure the value of $\mathcal{R}$ independently for each region of the Dalitz plot, and we find that it is significantly dependent on it.

3.4 Branching Fraction Analysis

The branching fractions are calculated according to

$$\mathcal{B} = \frac{N_1 - \mathcal{R}N_2}{N_{B\overline{B}} \times \epsilon} \tag{1}$$

where N_1 is the number of candidates in the signal region (SR) for on-resonance data; N_2 is the number of candidates in on-resonance data observed in the sideband region (GSB), so that $\mathcal{R}N_2$ is the estimated number of background candidates in the signal region; $N_{B\overline{B}}$ is the number of $B\overline{B}$ pairs produced and ϵ is the signal efficiency. The GSB is specified by $5.21 < m_{\rm ES} < 5.25\,{\rm GeV}/c^2$, $|\Delta E - \langle\Delta E\rangle\,| < 0.1\,{\rm GeV}$, where $\langle\Delta E\rangle$ is the mean value of ΔE for B meson decays found in calibration samples.

The numbers and distributions of candidates within the signal region remained unknown to us until all aspects of the analysis were finalized. The final selection criteria were chosen to maximize the sensitivity to the signal. Once chosen, neither the background description nor the cuts were changed. This procedure was followed independently for each channel.

For the signal efficiency in Eq. 1, we used simulated signal events and the same selection criteria as used for the data. The efficiencies due to π^0 reconstruction, particle identification, and ΔE selection criteria are determined from independent control samples derived from the data.

We have adopted two slightly differing approaches to the definition of selection efficiencies in Eq. 1. For the $B^0 \to \rho^\mp\pi^\pm$ and $B^0 \to \rho^0\pi^0$ measurements, we simulate the ρ resonances according to a non-relativistic Breit-Wigner distribution within the phase-space and with a $\cos^2\theta_H$ helicity distribution. For the non-resonant $B^0 \to \pi^+\pi^-\pi^0$ measurement, we simply assume a uniform distribution in phase-space, and ignore interferences. In these cases, we take as the denominator in the definition of the selection efficiency, the number of events generated in the full Dalitz plot, so that the loss of events outside our analysis cuts is compensated in Eq. 1. This provides a conventional branching fraction, having assumed a signal distribution, and ignoring interferences. By contrast, for the measurements in the remainder of the Dalitz plot, we have no a priori model of the dynamical distribution of events in phase space or of the feedthrough between different modes (other than of $B^0 \to \rho^\mp\pi^\pm$, whose rate is known), so we simulate the events according to a uniform distribution in phase space. We note that this introduces no systematic error, provided that the efficiency is flat over the region. We have verified that this is the case within the statistics available to us (the efficiency away from the kinematic boundaries, projected onto either Dalitz plot axis is consistent with a linear dependence, and the slope has been shown to be zero within errors of magnitude $\pm 3 \times 10^{-4}\,\mathrm{GeV}^{-2}$). In these cases, we take as our denominator for the efficiency calculation, only those events generated within the boundary of the defined region. In this way, events lying outside this boundary are not considered part of the signal. For these latter "topological" branching fractions, the measurement should be considered the total rate within the defined boundaries, not just that associated with any single resonance. If a signal were found, more work would be needed to determine the detailed dynamics.

3.5 Charge Asymmetry in $B^0 \to \rho^\mp\pi^\pm$

In principle, there are four decay rates that we could measure for the generic $B^0 \to \rho^\mp\pi^\pm$ mode: we define

$$\Gamma(B^0 \to \rho^+\pi^-) = \Gamma_{\rho\pi} \;;\; \Gamma(B^0 \to \rho^-\pi^+) = \Gamma_{\pi\rho} \tag{2}$$

and their CP conjugates

$$\Gamma(\overline{B}^0 \to \rho^-\pi^+) = \overline{\Gamma}_{\rho\pi} \;;\; \Gamma(\overline{B}^0 \to \rho^+\pi^-) = \overline{\Gamma}_{\pi\rho} \tag{3}$$

respectively. In the general, CP-violating case, all four are different, and there are two observable direct CP violations:

$$\begin{aligned} \Delta_{\rho\pi} = (\Gamma_{\rho\pi} - \overline{\Gamma}_{\rho\pi}) &\neq 0 \\ \text{and } \Delta_{\pi\rho} = (\Gamma_{\pi\rho} - \overline{\Gamma}_{\pi\rho}) &\neq 0. \end{aligned} \tag{4}$$

In the present analysis, we have not implemented tagging, but we have divided our $B^0 \to \rho^\mp\pi^\pm$ sample into two sub-samples, containing respectively the events with $\rho^+\pi^-$ and those with $\rho^-\pi^+$.

Using these, we may form the charge asymmetry:

$$\mathcal{A} = \frac{N(\rho^+\pi^-) - N(\rho^-\pi^+)}{N(\rho^+\pi^-) + N(\rho^-\pi^+)} \simeq \mathcal{A}_{\rm phys} + \mathcal{A}_{\rm det} \tag{5}$$

where $\mathcal{A}_{\rm det}$ is any detector-induced charge bias and

$$\mathcal{A}_{\rm phys} = \frac{(\Gamma_{\rho\pi} + \overline{\Gamma}_{\pi\rho}) - (\overline{\Gamma}_{\rho\pi} + \Gamma_{\pi\rho})}{(\Gamma_{\rho\pi} + \overline{\Gamma}_{\pi\rho}) + (\overline{\Gamma}_{\rho\pi} + \Gamma_{\pi\rho})}. \tag{6}$$

The numerator of Eq. 6 is simply the difference of the two direct CP violations in Eq. 4. If it is non-zero, it confirms direct CP-violation in at least one of the decays, Eqs. 2 and 3. We may assume that systematics due to background subtraction and luminosity cancel in the numerator of Eq. 5. Detector charge biases from tracking and from particle identification cuts were measured in an independent study with control samples of identified $D^+ \to K^0_S\pi^+$ events. Single $\pi^\pm$ charge asymmetries were limited to $< 2\%$, so we conservatively set a $\pm 2\%$ systematic uncertainty on our asymmetry measurement.

4 Treatment of Experimental Uncertainties

The systematic errors associated with branching fraction measurements arise from uncertainties in the background subtraction, in the overall signal efficiency and in the overall normalisation $N_{B\overline{B}}$.

In general, there are two contributions to the background subtraction: continuum backgrounds and B-related backgrounds. The estimate of the continuum background is given as the product of the number of events in the GSB and the factor $\mathcal{R}$, which is the estimated ratio of the number of background events in the GSB to that in the signal region, and is "measured" with sidebands and off-resonance running as described above. The number of events observed in the GSB has only a statistical error, which is taken into account mode-by-mode. The factor $\mathcal{R}$ has a systematic error given by the error in the fitted ARGUS shape parameter, ξ. This is taken into account independently for each mode.

Possible sources of B-related backgrounds include events with low-multiplicity decays to charm, which have been excluded explicitly by cuts in the Dalitz plot, and other charmless decays. The latter have been dealt with by counting the numbers found in the signal region in a dedicated charmless B decay "cocktail" simulation, scaling them according to the relative luminosities in data and simulation samples, and subtracting the appropriate numbers of events from the numbers in the signal region. We include relevant statistical errors from the simulation sample, and conservatively set the systematic error in this subtraction to be equal to the number subtracted.

We measure the overall signal efficiency ϵ with signal Monte Carlo simulation, and some uncertainty arises from limited signal mode statistics. The fractional error from this source is 2.7% in the $B^0 \to \rho^\mp\pi^\pm$ mode. In the other modes, this error is negligible compared to other sources of uncertainty, which are generally larger than the observed signals. The accuracy of the simulation is subject to systematic uncertainties including the tracking efficiency, calorimetric shower efficiency, particle identification efficiency and the interaction of selection requirements with the resolution accuracy of the simulation. At present the dominant uncertainties are in the particle identification, π^0 reconstruction, and ΔE and event-shape modelling in the simulation.

A discrepancy between the measured track-finding efficiency, and that obtained in our simulation is taken into account with a momentum-dependent weight per track. The uncertainty in

the determination of these weights leads to an uncertainty in the tracking efficiency of 1.2% per track, added coherently for both tracks used in the analyses. For π^0 reconstruction efficiency, we provide an energy-dependent weight, which is averaged over all accepted candidates in our signal simulation samples to provide a sample-dependent weight. We conservatively assign a systematic uncertainty of 5% per π^0 to this weight. The $\pi^\pm$ particle identification efficiency was measured in data with a $\pi^\pm$ control sample. It was found to be significantly smaller than that predicted in the simulation, and this difference is taken into account with a factor $R^{corr} = 0.948 \pm 0.018$, per $\pi^\pm$, added coherently for both pions.

A control sample of $B^+ \to \overline{D}^0\rho^+ \to K^+\pi^-\pi^+\pi^0$, which has similar kinematics to our modes, has been used to show that the simulation models the ΔE shape of such signals quite well. However, due to statistical limitations in this method we ascribe a systematic uncertainty of 5% to the signal efficiency from our simulation, to account for possible resolution differences on the order of 5 MeV in ΔE. Such uncertainties in the $m_{\rm ES}$ selection efficiency are negligible by comparison. For event shape cuts, the uncertainty on the efficiency has been taken as 5%.

The overall normalisation, $N_{B\overline{B}}$, comes from a dedicated "B-counting" study, which was made to determine the number of B mesons in the data samples. The final systematic error on this was determined to be 1.6%.

The overall systematic uncertainty is the sum in quadrature of the contributions from all sources. Table 2 shows a summary of sources and magnitudes of systematic errors.

Table 2: Summary of Systematic Error Sources and Magnitudes.

Source of Uncertainty	Uncertainty as % of Result	
	$B^0 \to \rho^\mp\pi^\pm$	Other modes
Background subtraction:		
$\mathcal{A}$	5.2	> 10
B-related Backgrounds	5.8	> 20
sub-total	7.8	> 30, dominant
MC Statistics	2.7	negligible
MC Efficiency Corrections	10.5	negligible
B-counting	1.6	1.6
Total	14.5	> 30

5 Results

Our preliminary measurements of branching fractions are summarized in Table 3. In calculating the upper limits, we have used the classical method outlined in [11]. In order to take account of the systematic errors, we have reduced the background estimate and the efficiency by one standard deviation (systematic) before making the calculation.

The new value for the $B^0 \to \rho^\mp\pi^\pm$ branching fraction is more precise than previous measurements. Our upper limit for $B^0 \to \rho^0\pi^0$ is consistent with Standard Model expectations [12]. Our

Table 3: Results for the 3π final state analyses. We aggregate the first two columns to obtain the branching fraction for $B^0 \to \rho^{\pm}\pi^{\mp}$ (the asymmetry is calculated independently.)

Quantity	$B^0 \to \rho^+\pi^-$	$B^0 \to \rho^-\pi^+$	$B^0 \to \rho^0\pi^0$	$B^0 \to \pi^+\,\pi^-\,\pi^0$ (NR)
$\cos\theta_T$	< 0.75	< 0.75	< 0.65	< 0.85
Fisher	< 0.75	< 0.75	< 0.65	< 1.1
π^0 mass GeV/c^2	0.110-0.160	0.110-0.160	0.115-0.155	0.115-0.155
events in SR				
On-res data	121	118	27	41
Off-res data	11	12	5	3
events in GSB				
On-res data	590	540	142	362
Off-res data	74	74	24	46
$\mathcal{A}$	0.128 ± 0.005	0.128 ± 0.005	0.132 ± 0.012	0.116 ± 0.006
$q\overline{q}$ BG in SR	$75.5 \pm 3.1 \pm 3.0$	$69.1 \pm 3.0 \pm 2.7$	$18.7 \pm 2.2 \pm 1.7$	$42.0 \pm 3.1 \pm 2.0$
$b\overline{b}$ BG in SR	$2.7 \pm 1.6 \pm 2.7$	$2.7 \pm 1.6 \pm 2.7$	$2.2 \pm 1.5 \pm 2.2$	$3.2 \pm 1.8 \pm 3.2$
Signal	$42.8 \pm 11.5 \pm 4.0$	$46.2 \pm 11.4 \pm 3.8$	$6.1 \pm 5.8 \pm 2.8$	$-4.2 \pm 7.3 \pm 3.8$
Signal Efficiency	0.135 ± 0.016		0.074 ± 0.009	0.075 ± 0.010
Stat. signif. (σ)	5.01		0.96	N/A
$\mathcal{B}$ $(\times 10^{-6})$	$28.9 \pm 5.4 \pm 4.3$		$3.6 \pm 3.5 \pm 1.7$	N/A
90% CL limit $(\times 10^{-6})$	N/A		< 10.6	< 7.3

upper limit of 7.3×10^{-6} for non-resonant $\pi^+\pi^-\pi^0$ decay ignores interference effects, an approach similar to that adopted by CLEO [13] for non-resonant B^+ decays to three charged pions.

In addition, we have made a preliminary measurment of the CP asymmetry defined in Eq. (6) and find

$$\mathcal{A}_{\rm phys} = -0.04 \pm 0.18 \pm 0.02, \tag{7}$$

consistent with zero. This does not however indicate that there is no direct CP violation in $B^0 \to \rho^\mp\pi^\pm$ decays, as the measured quantity is the difference between two direct CP violations, and we cannot exclude the possibility of a (coincidental) cancellation of the two.

The signal for $B^0 \to \rho^\mp\pi^\pm$ can be seen in the distributions of $m_{\rm ES}$ and ΔE shown in Fig. 2. The results for the topological branching fractions are given in Table 4. The existence of a slight,

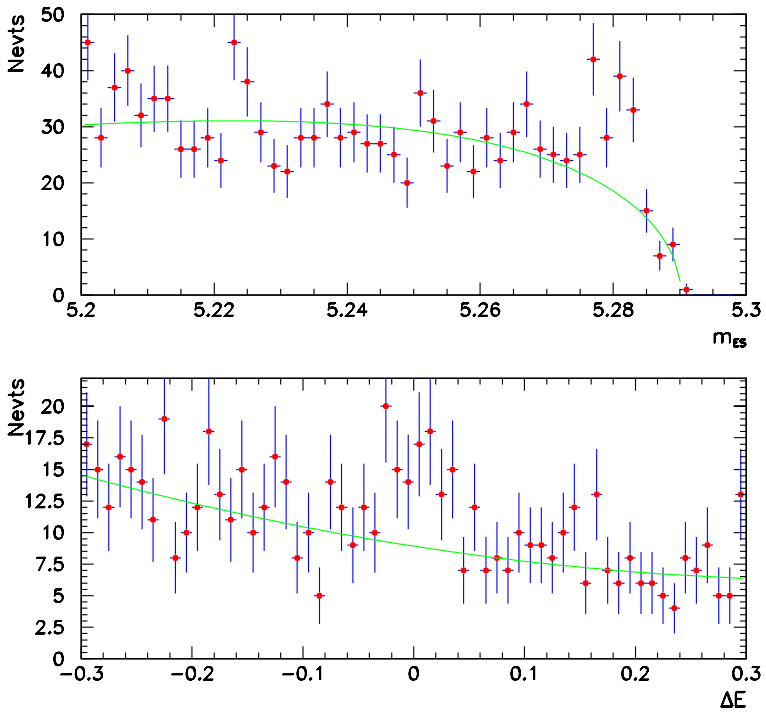

Figure 2: $m_{\rm ES}$ and ΔE distributions for $B^0 \to \rho^\pm\pi^\mp$. The signal region requirement was made on the orthogonal variable in each case.

though not statistically significant excess in Region III could be a hint of structure due to higher resonances, such as the $\rho'^\pm(1450)$. This would have implications for the measurement of α [14]. Further data are necessary to confirm whether this effect is real.

Region VI is sensitive to the scalar resonance $f_0(400-1200)$, proposed as a significant contribution in this region [4]. Our sensitivity has not yet reached that required to test this possibility.

We can get an impression of the whole Dalitz plot from Fig. 3, which shows the full Dalitz plot area for various samples. Fig. 3 a) shows the distribution of the data in phase space after the

Table 4: Results for the 3π final state analyses.

Quantity	Region III	Region IV	Region V	Region VI
$\cos\theta_T$	< 0.75	< 0.65	< 0.75	< 0.55
Fisher	< 0.75	< 0.70	< 0.75	< 0.40
π^0 mass GeV/c^2	0.110-0.160	0.115-0.155	0.110-0.160	0.115-0.155
events in SR				
On-res data	75	8	44	6
Off-res data	4	2	0	0
events in GSB				
On-res data	390	80	268	22
Off-res data	54	6	38	2
$\mathcal{A}$	0.131 ± 0.006	0.134 ± 0.011	0.132 ± 0.009	0.142 ± 0.017
$q\overline{q}$ BG in SR	$51.1 \pm 3.7 \pm 2.4$	$10.7 \pm 1.7 \pm 0.8$	$35.4 \pm 3.1 \pm 2.3$	$3.1 \pm 0.9 \pm 0.4$
$b\overline{b}$ BG in SR	$6.5 \pm 2.5 \pm 6.5$	$2.0 \pm 1.4 \pm 2.0$	0	$3.2 \pm 1.8 \pm 3.2$
Signal	$17.4 \pm 9.7 \pm 6.9$	$-4.7 \pm 3.6 \pm 2.2$	$8.6 \pm 7.3 \pm 2.3$	$-0.3 \pm 3.2 \pm 3.2$
Signal Efficiency	0.150 ± 0.021	0.087 ± 0.018	0.150 ± 0.023	0.067 ± 0.014
Stat. signif. (σ)	1.83	N/A	0.40	N/A
$\mathcal{B}$ ($\times 10^{-6}$)	$5.1 \pm 2.9 \pm 2.2$	N/A	$2.5 \pm 2.1 \pm 0.8$	N/A
90% CL limit ($\times 10^{-6}$)	< 11.3	< 2.7	< 6.1	< 5.2

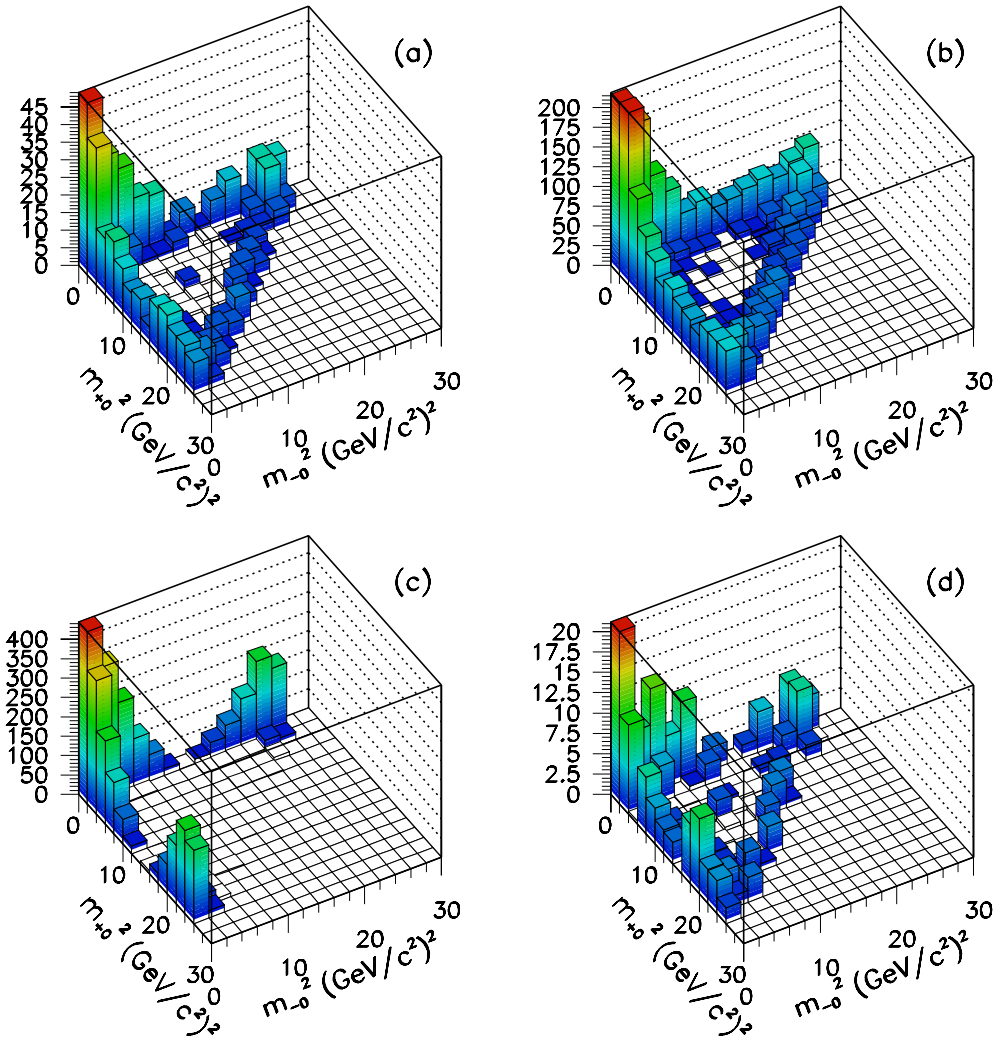

Figure 3: Dalitz plots for $B^0 \to \pi^+\pi^-\pi^0$ after $B^0 \to \rho^\mp\pi^\pm$ analysis requirements (except $m_{\pi\pi}$ and $|\cos\theta_H|$): (a) data SR, (b) data GSB, (c) Monte Carlo SR, (d) background-subtracted data SR.

.

analysis cuts are applied, and Fig. 3 b) shows the background distribution measured in the GSB. Figure 3 c) shows an example Monte Carlo signal and Fig. 3 d) shows the background-subtracted signal. The helicity structure is clearly visible along the two $\rho^{\pm}$-bands in the background-subtracted figure. The peak near the origin (*ie.* low π^0 energy), even after background subtraction, indicates an efficiency enhancement in real signal events (also present in the simulated signal sample), in which events missing one low-energy photon due to acceptance effects are recovered by combinatorial substitution of a different photon. This effect significantly enhances the population of signal events at low π^0 energies (only one candidate is accepted per event).

6 Conclusion

We have made a number of preliminary measurements of branching fractions into regions of the $B^0 \to \pi^+\pi^-\pi^0$ Dalitz plot. In particular, a new measurement of the $B^0 \to \rho^{\mp}\pi^{\pm}$ branching fraction, upper limits for the $B^0 \to \rho^0\pi^0$ mode and non-resonant $B^0 \to \pi^+\pi^-\pi^0$, and four upper limit measurements of topological branching fractions into other regions of the Dalitz plot have been reported. We have also made the a preliminary measurement of the direct CP-violating asymmetry between the rates of untagged $\rho^+\pi^-$ and $\rho^-\pi^+$, finding no significant evidence for an effect.

7 Acknowledgments

We are grateful for the extraordinary contributions of our PEP-II colleagues in achieving the excellent luminosity and machine conditions that have made this work possible. The collaborating institutions wish to thank SLAC for its support and the kind hospitality extended to them. This work is supported by the US Department of Energy and National Science Foundation, the Natural Sciences and Engineering Research Council (Canada), Institute of High Energy Physics (China), the Commissariat à l'Energie Atomique and Institut National de Physique Nucléaire et de Physique des Particules (France), the Bundesministerium für Bildung und Forschung (Germany), the Istituto Nazionale di Fisica Nucleare (Italy), the Research Council of Norway, the Ministry of Science and Technology of the Russian Federation, and the Particle Physics and Astronomy Research Council (United Kingdom). Individuals have received support from the Swiss National Science Foundation, the A. P. Sloan Foundation, the Research Corporation, and the Alexander von Humboldt Foundation.

References

[1] P.F. Harrison and H.R. Quinn (eds.) [The *BABAR* Collaboration], "The *BABAR* Physics Book", SLAC-R-504, 1998.

[2] C.P. Jessop *et al.,* [The CLEO Collaboration], Phys. Rev. Lett. **85** 2881, 2000.

[3] A. Deandrea et al. Phys. Rev. **D62** 036001, 2000.
A. Deandrea et al. Phys. Rev. **D62** 114011, 2000.

[4] A. Deandrea and A. D. Polosa, Phys. Rev. Lett. **86** 216, (2001).

[5] A. Palano *et al.,* [The *BABAR* Collaboration], to appear in Nucl. Instrum. Methods [hep-ex/0105044].

[6] H. R. Quinn and J. P. Silva, Phys. Rev. D **62**, 054002 (2000) [hep-ph/0001290].

[7] A. Bozek *et al.,* [The Belle Collaboration], hep-ex/0104041.

[8] T. J. Champion *et al.,* [The *BABAR* Collaboration], hep-ex/0011018.

[9] D. M. Asner *et al.,* [The CLEO Collaboration], Phys. Rev. **D53**, 1039 (1996).

[10] H. Albrecht *et al.,* [ARGUS Collaboration], "Search For Hadronic B $\rightarrow$ U Decays," Phys. Lett. B **241**, 278 (1990).

[11] R.M. Barnett et al., Phys. Rev. **D54** 1, (1996).

[12] See eg. A. Ali, G. Kramer, Cai-Dian Lu Phys. Rev. **D58**, 094009 (1998).

[13] T. Bergfeld et al. Phys. Rev. Lett. **77**, 4503, (1996).

[14] S. Versille, PhD thesis (in French), http://www-lpnhep.in2p3.fr/babar/public/versille/Thesis/